# Reactivity of Intermetallic Compounds: A Solid State Approach to Direct Reactions of Silicon

**Jörg Acker*,† and Klaus Bohmhammel‡**

*Princeton University, Department of Chemistry, Princeton, New Jersey 08544, and Freiberg University of Mining and Technology, Department of Physical Chemistry, D-09599 Freiberg, Germany*

*Received: August 7, 2001; In Final Form: February 16, 2002*

The present work is focused on a new approach to describe, quantify, and compare the reactivity of various transition metal silicide phases toward hydrogen chloride. Thermodynamic and kinetic parameters are obtained from isothermal calorimetric studies of these reactions. The reactivity of the silicide phases is discussed in terms of reaction start temperatures, rate constants, and apparent activation energies. Negative apparent activation energies are observed at low temperatures and are attributed to an initial stage of reaction where chlorine is chemisorbed and then incorporated into the silicide lattice near the surface. At a later time, a chlorine-containing reaction layer is formed having a composition and reactivity remarkably different from that of the bulk phase. On the basis of solid-state investigations, a diffusion model of the microscopic structure of these layers is presented, where a displacement of nickel atoms occurs followed by the occupation of nickel sites by chlorine. A model is suggested in which the electron level of the reaction layer is adjusted by the chlorine content of this layer, resulting in a electronic stabilization of silylenoide species at the surface. The model is applied to explain product distribution in the induction period during the direct reaction of silicon and methyl chloride.

## Introduction

The present work deals with the question of how a binary alloy constituent A influences the reactivity of alloy constituent B if B is selectively removed from the binary alloy by reaction with a gaseous compound. In particular, this work is focused on the heterogeneous reaction of hydrogen chloride and various transition metal silicide phases where silicon is removed as dichlorosilane, trichlorosilane, and silicon tetrachloride.

Heterogeneous reactions of intermetallic compounds show characteristic features for heterogeneous bimetallic catalysis where the concepts of surface segregation of one alloy constituent at the surface, spill-over processes, and altered adsorption and reaction properties due to alloying the constituents were introduced.[1] Furthermore, features for oxidation of alloys are also appearing, introduced as concepts of solid metal oxide layer formation, ion conductivity of the reaction layer, internal oxidation of the less noble alloy constituent, and solubility of oxygen in one or both constituents.[2]

When dealing with transition silicides, it is important to note that silicon can be removed from the solid phase in the form of various chlorosilanes. The silane chlorine content depends on the transition metal that is used as well as on the metal-to-silicon ratio of the reacting solid phase. The depletion of silicon changes the solid-phase composition, which alters the reactivity of the solid phase and the product distribution. As a consequence, a thermodynamically defined starting point and a defined ending point are urgent conditions for reliable and comparable results. Pure silicide phases are used as staring materials to fulfill the first demand. Also, the reaction conditions have to be chosen in such a way that silicon is removed only to a small extent from the studied silicide phases. Because of the small changes in composition during the reaction, the measured kinetic and thermodynamic reaction parameters can be attributed to the pure silicide phase. This serves as the necessary precondition for correlation of the reaction parameters to thermodynamic functions of pure phases and to the discussion of differences between various metals or different metal-to-silicon ratios of pure phases quantitatively.

Our approach to investigate the reactivity of transition metal silicides is split into two levels. On a macroscopic level, the reactivity of the studied silicide phases is described in terms of reaction start temperatures, rate constants, activation energies, and product distribution in relation to thermodynamic functions of pure silicide phases. On a microscopic level, processes near and on the silicide surface are discussed in light of diffusion phenomena and surface reactions.

In the following section, the background and previous studies are presented. The two major processes of industrial silicon chemistry are the reactions of silicon with either methyl chloride or hydrogen chloride, which are known as direct reactions of silicon.[3−7] They are unique examples of how the reactivity of silicon can be controlled by the addition of various metals. In direct synthesis, methyl chloride is passed over a silicon−copper mixture at temperatures between 250 and 320 °C. The main product is dimethyldichlorosilane, which is the basic compound for silicone production. The second reaction is the hydrochlorination reaction where technical grade silicon, containing numerous metallic and nonmetallic impurities, reacts with hydrogen chloride. Trichlorosilane is the major product and is used for manufacturing solar grade and semiconductor grade silicon.

A third reaction belongs to the same class of metal-controlled reactions: the silicide-assisted conversion of silicon tetrachloride

* Author to whom correspondence should be addressed. New address: Leibniz Institute for Solid State and Materials Research Dresden, P.O. Box 27 01 16, D-01171 Dresden, Germany. Email: j.acker@ifw-dresden.de.
† Princeton University.
‡ Freiberg University of Mining and Technology.

10.1021/jp0130315 CCC: $22.00 
Published on Web 04/18/2002

**TABLE 1: Direct Synthesis Metal Catalysts and Product Distributions**[a]

| catalyst | main product | product distribution (mol %) | secondary product | product distribution (mol %) | estimated M−Cl bond energy (kJ mol$^{-1}$) |
|---|---|---|---|---|---|
| Pb | $CH_3HSiCl_2$ | 75 | $HSiCl_3$ | 10 | 272 |
| Cu | $(CH_3)_2SiCl_2$ | 85 | $CH_3SiCl_3$ | 10 | 326 |
| Sn | $CH_3SiCl_3$ | 85 | $SiCl_4$ | 10 | 356 |
| Fe | $CH_3SiCl_3$ | 85 | $(CH_3)_2SiCl_2$ | 10 | 372 |
| Si | $HSiCl_3$ | 70 | $CH_3HSiCl_2$ | 20 | 381 |
| Ca | $(CH_3)_3SiCl$ | 60 | $(CH_3)_2SiCl_2$ | 15 | 431 |

[a] This table is taken from Falconer et al.[12]

**TABLE 2: Metals and Product Distributions in the Hydrodechlorination Reaction**

| metals | solid products | gaseous products | ref |
|---|---|---|---|
| Fe, Co, Ni | silicide phases | $HSiCl_3$ | 9, 10, 13 |
| Cu | silicide phases and CuCl | $H_2SiCl_2$ and $HSiCl_3$ | 9, 10, 13 |
| Mn, Cr | metal chlorides[a] | $HSiCl_3$ | 13 |
| Mg | $MgCl_2$ | $SiH_4$ and $HSiCl_3$ | 14 |
| La, Y | nanocrystalline Si and metal chlorides | $HSiCl_3$ | 15 |

[a] Volatile under reaction conditions.

into trichlorosilane (eqs 1 and 2). Here, a gaseous mixture of silicon tetrachloride and hydrogen is passed over a desired transition metal.[8−10] During an induction period, silicon tetrachloride is almost completely consumed by the metal under the formation of the silicide phase, which is thermodynamically stable at given reaction temperature (eq 1).

$$x\mathrm{SiCl_4} + 2x\mathrm{H_2} + \mathrm{M} \rightarrow \mathrm{MSi}_x + 4x\mathrm{HCl} \qquad (1)$$

Once a silicide phase has been established, the conversion of silicon tetrachloride into trichlorosilane starts (eq 2).

$$\mathrm{SiCl_4} + \mathrm{H_2} \rightarrow \mathrm{HSiCl_3} + \mathrm{HCl} \qquad (2)$$

The most remarkable feature of this reaction is that silicon atoms of the silicide phase are continuously depleted by reaction with hydrogen chloride (yielding trichlorosilane) and continuously restored by silicon deposition from the gas phase (by the reaction of silicon tetrachloride and hydrogen) at the same time. The mechanism in principle is the same as that described for the catalytic activity of $RuO_2(110)$ in a CO oxidation reaction in which oxygen lattice atoms reacting with CO are restored by the gas phase.[11]

Tables 1 and 2 illustrate the wide range of product distribution for a variety of metals during direct synthesis and hydrodechlorination reactions, respectively. Table 1 is taken from Falconer's work of 1985.[12]

As the most recent results, the influence of a metal on the product distribution of the hydrodechlorination reaction should be discussed in more detail. Similar to Falconer,[12] who correlated the obtained product distributions to metal−chlorine bond strength, we correlate the product distribution of the hydrodechlorination reaction to the free enthalpy (Gibbs function) of metal chloride formation (Table 3).

With increasing negative free enthalpy of metal chloride formation, the ability to substitute the chlorine atoms of silicon tetrachloride by hydrogen atoms and even by silicon atoms increases. La and Y were found to form silicon nanoclusters;[15] metals such as Cr or Mn form stable, but under our reaction conditions, volatile chlorides;[13] and Fe, Co, Ni, and Pt belong to one group[9,10,13] and form trichlorosilane. Taking into account

**TABLE 3: Free Energies of Formation ($\Delta_f G$) of Metal Chlorides**[16]

| compound | $\Delta_f G$ (kJ mol$^{-1}$) | compound | $\Delta_f G$ (kJ mol$^{-1}$) |
|---|---|---|---|
| $PtCl_2$ | −93.248 | $CrCl_2$ | −356.209 |
| $CuCl_2$ | −173.810 | $ZnCl_2$[a] | −369.362 |
| CuCl | −138.089 | $MnCl_2$ | −440.489 |
| $NiCl_2$ | −259.151 | $MgCl_2$ | −592.086 |
| $CoCl_2$ | −269.661 | $CaCl_2$ | −748.123 |
| $SnCl_2$[a] | −286.233 | $YCl_3$ | −927.754 |
| $FeCl_2$ | −302.354 | $CeCl_3$ | −978.066 |
| $PbCl_2$[a] | −314.122 | $LaCl_3$ | −995.389 |

[a] No silicide phases formed.

only the metals that are able to form silicide phases, the results in Tables 1 and 2 are similar in the manner of instigating the attachment of hydrogen atoms or methyl groups to silicon.

Copper, the most effective metal to form products of industrial need, is one exception. The free enthalpies of CuCl and $CuCl_2$ formation are smaller than that for $PtCl_2$ formation and larger than that for $NiCl_2$ formation. Platinum and nickel form trichlorosilane, but copper forms dichlorosilane. The second exception is found between magnesium silicide and calcium silicide in both reactions. In direct synthesis, calcium does not form $Si(CH_3)_4$; however, magnesium in the hydrodechlorination reaction produces $SiH_4$. The silicide phases of these metals should exhibit a similar ionicity. The differences in the reactivity between calcium and magnesium in the direct synthesis and in the hydrodechlorination reaction, respectively, can be explained by differences in acid−base strength between methyl chloride and the silicon tetrachloride/hydrogen mixture. A comparable scale of oxidation strength is known from the treatment of calcium silicides with hydrochloric acid at different concentrations and temperatures that produces different layered silicon compounds.[17−19]

From the overwhelming number of papers dealing with direct reactions of silicon, four topics of research on the mechanism of direct reactions have to be considered for their importance to the present study. Lewis et al.[20] found evidence of intermediacy of a $CH_3SiCl$ silylene species in direct synthesis, a finding that was later confirmed by several groups.[9,10,21,22] Falconer et al.[23] and Lewis et al.[24] discovered silicon segregation at the surface of $Cu_3Si$ samples after exposing the samples to methyl chloride. Zinc, an effective promoter in direct synthesis and an alloy in copper silicide samples, was found to enhance silicon segregation. Therefore, the silicon-enriched surface was considered to be the active phase in direct synthesis.[24−26] Falconer et al.[27−29] studied the induction period of direct synthesis extensively and established a detailed view of the reactive sites, which are always related to the presence of chlorine at the surface. Auger electron spectroscopy studies on copper−silicon alloy samples revealed the existence of Si−Cl (and Si−C) bonds, which is coincidental to a weakening of the Cu−Si bonds.[12] Finally, Roewer and Walter discovered the presence of chlorine in the bulk of transition metal silicide phases, which were active in the conversion of silicon tetrachloride to trichlorosilane.[9,10]

These results suggested that chlorine bound on the surface or incorporated into a silicide bulk phase is necessary to make the solid phase reactive. Therefore, the nickel−silicon−chlorine system was extensively studied by means of a model reaction. It was found that the reaction of a nickel silicide phase and nickel(II) chloride (eq 3) having a water content of about 1 wt % is a convenient model for the reaction of hydrogen chloride and a nickel silicide phase.[30] The reaction has to proceed in a closed reaction system to retain all gaseous products involved

**TABLE 4: Transition Metal Silicide Chlorides and Their Structural Features[a]**

| compound | ionic formulation | structural features | ref |
|---|---|---|---|
| $Gd_4I_5Si$ | $(Gd^{3+})_4(I^-)_5Si^{4-}\cdot 3e^-$ | | 33 |
| $Gd_3I_3Si$ | $(Gd^{3+})_3(I^-)_3Si^{4-}\cdot 2e^-$ | | 33 |
| MISi, M = La, Ce, Pr | $(La^{3+})(I^-)\,[Si(3b)^-]\cdot 1e^-$ | 1.0 $e^-$/Si: $Si_6$ rings | 34, 35 |
| $La_5I_3Si_5$ | $(La^{3+})_5(I^-)_3\,[Si(2b)^{2-}]_4[Si(3b)^-]\cdot 3e^-$ | 1.80 $e^-$/Si: $Si_{22}$ rings | 34, 35 |
| $La_4I_3Si_4$ | $(La^{3+})_4(I^-)_3\,[Si(2b)^{2-}]_2\,[Si(3b)^-]_2\cdot 3e^-$ | 1.50 $e^-$/Si: $Si_6$- and $Si_{14}$ rings | 34, 35 |
| $La_3Cl_2Si_3$ | $(La^{3+})_3(Cl^-)_2[Si(2b)^{2-}]_3\cdot 1e^-$ | 2.00 $e^-$/Si: Si zigzag chains | 35 |
| $La_6Br_3Si_7$ | $(La^{3+})_6(Br^-)_3[Si(2b)^{2-}]_5[Si(3b)^-]_2\cdot 3e^-$ | 1.71 $e^-$/Si: $Si_{12}$ rings | 35 |

$e^-$/Si = the number of electrons formally transferred to silicon.

for subsequent reactions.

$$NiSi_m + nNiCl_2 \rightarrow Ni_{1+n}Si_{m-0.5n}(Cl) + 0.5nSiCl_4 \quad (3)$$

This reaction was studied in detail by thermokinetic measurements, in situ X-ray powder diffraction measurements, and in situ IR spectroscopy gas-phase analysis.[13,30,31] By dehydratation of nickel(II) chloride (containing 1 wt % water), a very low hydrogen chloride partial pressure is built up, and the reaction proceeds less rigorously than it does under a hydrogen chloride partial pressure of 1 bar. At temperatures below 350 °C, hydrogen chloride chemisorbs on the silicide phase. Above 350 °C, the chemical reaction between the silicide phase and chemisorbed hydrogen chloride starts, and silicon tetrachloride, trichlorosilane, and hydrogen are formed. By a parallel process, in the reaction system, hydrogen chloride is continuously regenerated by the reduction of nickel(II) chloride by hydrogen or trichlorosilane.[30,31] Silicide phases were prepared by reaction 3. In the solid bulk phase, chlorine was present in higher concentrations throughout the reactions than it was in the equilibrated solid products. The chlorine content in so-prepared nickel silicide phases depends on the metal-to-silicon ratio of the formed product silicide phase, on the silicon tetrachloride partial pressure during their synthesis, and on the reaction temperature.[30] With increasing chlorine content, an enlargement of the silicide phase unit cell was observed.[30] On the basis of the analytically determined chlorine contents, a thermodynamic model of the dilute solution of chlorine in nickel silicide phases based on nonspecific chlorine−silicide interaction was proposed, and the enthalpy and entropy of the chlorine intake processes were calculated.[32]

Yet unclear is the state of chlorine bonding in these silicide phases. It is definitely excluded that chlorine is present as a metal chloride. Moessbauer spectroscopic studies of chlorine-containing iron silicides showed that the presence of chlorine in these compounds disturbs the crystal field and slightly disturbs the lattice structure. But iron chlorides were never found.[30] To avoid any confusion about the bonding state of chlorine in these silicide phases, they are referred to as "chlorine-containing silicide phases".

Their most remarkably chemical property is their thermal decomposition starting above 200 °C, which forms breakdown products of elemental nickel, highly disordered $Ni_3Si$ or $Ni_5Si_2$ phases, and silicon tetrachloride.[30,31]

The thermal decomposition reveals the totally changed chemical properties of chlorine-containing silicide phases compared to those of pure silicide phases. Therefore, chlorine-containing silicide phases can be considered to be a distinct class of compounds. Meanwhile, numerous compounds consisting of a rare earth metal, silicon, and chlorine were synthesized and designated as transition metal silicide chlorides.[33−35] A summary of these compounds is given in Table 4.

## Experimental Section

**Preparation of the Silicides.** For the preparation of nickel and iron silicides, nickel (99.9%) or iron powders (99.8%) were mixed with silicon powder (99.9%) in certain ratios. To compensate for a loss of silicon by evaporation, an extra 1−2% of silicon was added (the values are based on our experience of our furnace system). The mixtures were heated under a constant argon flow (25 L $h^{-1}$) at a rate of 10 K $min^{-1}$ to a temperature of about 50 K above the melting point of the metal ($T_F$(Ni) = 1453 °C, $T_F$(Fe) = 1535 °C, $T_F$(Si) = 1410 °C). After holding samples at this temperature for 1 h, they were slowly cooled to 900 °C (5 K $min^{-1}$) and held for 7 h. After cooling to room temperature, the reguli were annealed in sealed, evacuated quartz ampules ($10^{-5}$ Torr) for 6 weeks at 900 °C. Analysis by X-ray powder diffraction (Siemens D5000) gave a diffraction pattern of the pure silicide phases. Slices were prepared from all samples and then polished and investigated by SEM-EDX. The deviations from the desired composition were below 0.2 at. %. $Cu_3Si$ was prepared by arc melting of semiconductor grade silicon (roughly crushed wafers) and copper (99.999%). The sample was melted and crushed five times and annealed in an evacuated ampule for 3 weeks at 770 °C. Phase purity was confirmed by X-ray powder diffraction. A copper−silicon−zinc alloy with a composition of $Cu_3Si$ + 1.5 at. % Zn (Zn 99.98%) was prepared in the same manner.

**Calorimetric Measurements.** Isothermal thermokinetic measurements were carried out in a differential scanning calorimeter (DSC-111, Setaram), a Tian−Calvet-type calorimeter. The reaction proceeds in a stainless steel flow cell having a gas inlet and outlet, also made from stainless steel. The sample cell (volume 0.125 mL) filled with a grained silicide sample (particle sizes between 50 and 300 $\mu$m) and the empty reference cell are both connected to a gas dosing system. A typical run starts by passing a constant argon flow through the cells (flow rates vary between 90 and 105 mL per hour) while heating them to the desired temperature. After establishing a stable baseline under isothermal conditions, a sample valve, taken from a gas chromatograph, is opened, and the argon flow carries a constant volume of dry hydrogen chloride gas (between 1 and 8 mL) into the sample cell. For each run, a new silicide sample was used.

Blank tests were performed to determine the heat and rate of passing hydrogen chloride into empty sample cells. The obtained peaks for the blank tests have totally different shapes compared to those for the silicide-filled cells. Depending on the choice of silicide phase and the sample mass, the heat of reaction for blank tests is between 1 and 6% of the heat of reaction for the silicides (Figure 1). Furthermore, it was found that the rate constant for the reaction of silicide and hydrogen chloride does not depend on the volume of hydrogen chloride gas that is introduced.

**Solid-State Investigations.** Polished nickel silicide slices reacted with hydrogen chloride under various partial pressures and temperatures. To study the reaction on the sample surface under mild conditions (i.e., under very low hydrogen chloride partial pressure), silicide samples were embedded in $NiCl_2$ (having 1 wt % $H_2O$) and heated to a preset temperature. After the reactions, the samples were broken into two pieces, and their

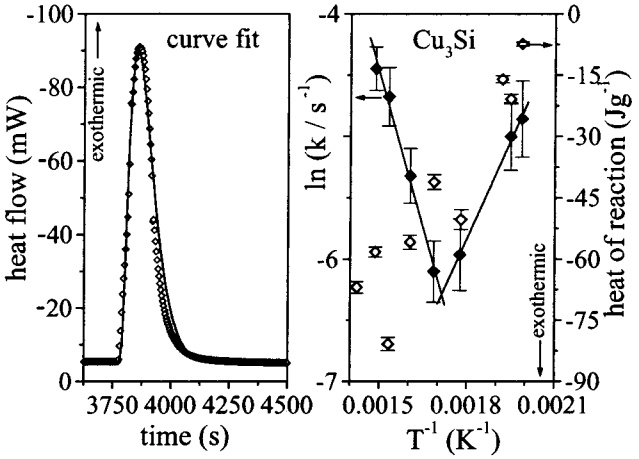


**Figure 1.** Fit of a heat-flow curve ($Cu_3Si$ + HCl) using the Avrami−Erofeyev equation (left) and rate constants and heat of reaction as function of inverse temperature (right).

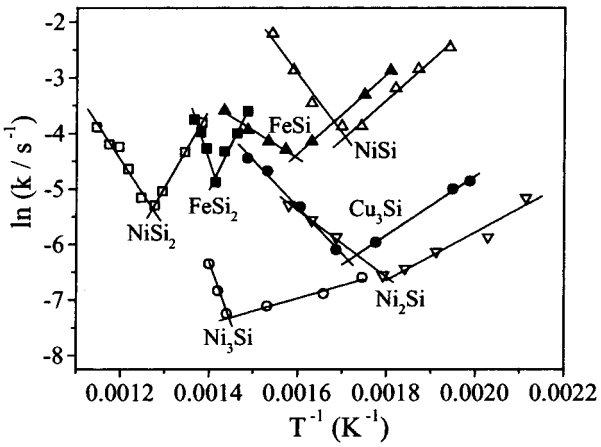


**Figure 2.** Arrhenius plot for the reactions of various metal silicide phases and hydrogen chloride.

cross sections were either polished or left as received. The samples were studied by scanning microscopy and EDX analysis (JEOL JSM 6400, EDX: Noran) and X-ray powder diffraction (Siemens D5000). Because of handling in air, chlorine is detected only by the penetration depth of the electron beam when chlorine is located below the surface. The obtained values are not considered to be representative and are omitted; therefore, only nickel-to-silicon ratios are discussed. Rutherford backscattering measurements were performed on a 4 MeV van de Graff accelerator at the State University Utrecht, Utrecht, The Netherlands.

**Thermokinetic Model.** The obtained heat-flow curves were fitted by the Avrami−Erofeyev equation (eq 4), a common thermokinetic approach that describes the formation and growth of 3-D spherical nuclei.

$$\text{rate} = \frac{\mathrm{d}q}{\mathrm{d}t} = q_{\text{total}} k^3 \left(\frac{1}{3} t^2 \mathrm{e}^{-(kt)^3}\right) \tag{4}$$

($\mathrm{d}q/\mathrm{d}t$ = heat flow, $q_{\text{total}}$ = heat of reaction, $t$ = time, $k$ = rate constant).

One should notice that only one rate constant $k$ is used to describe the whole process. Other than what is known from molecular reaction dynamics or kinetics of elementary steps, the rate constant cannot be attributed to a single reaction. Usually, no conclusion about the reaction mechanism can be drawn from thermokinetic models.

For the reaction of a silicide phase with hydrogen chloride, the rate constants as well as corresponding heats of reaction were obtained by fitting the Avrami−Erofeyev equation to the experimental curve. For each curve fit, the considered time scale is at least 6 times higher than the time constant of our DSC apparatus of 30 s; a deconvolution of the curve (desmearing) was not necessary (Figure 1). The error in the curve fitting of eq 4 is less than 5%, which was determined from the standard deviation. The reliability of the curve fits was tested by varying the number of points taken into account for curve fitting. A maximum deviation of the rate constant of 10% was obtained. Normally, the values are less than 8% (from the standard deviation).

An evaluation of heat flow curves by the Avrami−Erofeyev equation requires a widely uniform signal (Figure 1). This demand is consistently fulfilled for all thermokinetic data presented in this work. At higher temperatures (above the reaction temperatures discussed herein), the signal becomes too structured, shoulders appear, and peak splitting occurs. At this point, the applied thermokinetic model fails to evaluate the heat flow curves. A deconvolution of the signals fails because of the high interference and the lack of sufficient chemical background to establish a model, which describes the proceeding reactions or processes causing these structured signals.

## Results

**I. Thermokinetic and Thermodynamic Studies.** The measurements were carried out under the guidelines given in the Introduction. In all experiments, the amount of the silicide phase was, by a molar factor, 4 or 5 times higher than the amount of hydrogen chloride to make sure that the silicide phase was converted into the silicide phase having the adjacent higher metal content according to the phase diagram. After each run, the removed silicide sample was studied by X-ray powder diffraction. In all samples, only the adjacent silicide phase and the unreacted initial phase were found. Metal chlorides were never found. In the case of copper silicides, elemental copper was detected.

From the Arrhenius plot in Figure 2, it can be seen that all of the investigated silicide phases show a v-shaped activation energy pattern. At low temperatures, a negative activation energy is consistently found, which describes a decreasing reaction rate with increasing temperature. After passing through a minimum, the reaction rate increases with temperature, and a positive activation energy is observed. From the slope of the line fits, the activation energies were calculated. For a given silicide, the point of intersection of the line fits of positive and negative slopes corresponds to a temperature, referred to as the "reaction start temperature", on the $y$ axis; this point corresponds to the natural logarithm of a rate constant, which is called the "minimum rate constant" $\ln k_{\text{min}}$. Reaction start temperatures, minimum rate constants, and activation energies are listed in Table 5.

In all experiments, an induction period is observed in which the incoming hydrogen chloride is adsorbed, corresponding to a decrease and followed by an increase in pressure. This pressure drop lasts from a few seconds to few minutes. In blank tests with empty cells, this pressure change was never observed. Figure 3 compares four heat flow curves of the reaction of hydrogen chloride with $NiSi_2$, NiSi, $Ni_2Si$, and $Ni_3Si$, respectively. The curves are taken from the middle of the positive apparent activation energy region and normalized to the start of the reaction at time zero. A bar in each graph indicates how long hydrogen chloride is present in the flow cells (calculated from the flow rates). NiSi is the phase with the highest reaction

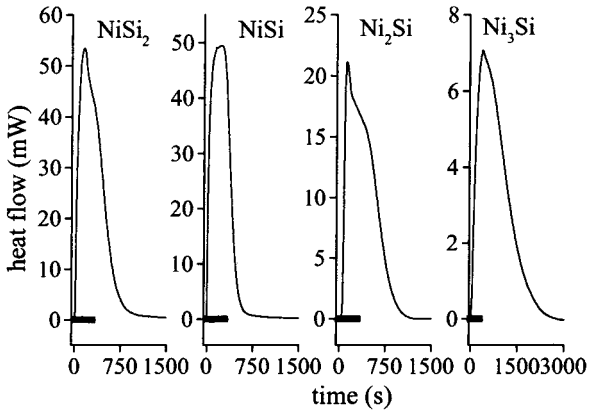


**Figure 3.** Heat-flow curves of the reaction of nickel silicide phases and hydrogen chloride taken from the middle of the positive activation energy branch. The bar indicates how long hydrogen chloride is present in the flow cells.

**TABLE 5: Apparent Activation Energies, Reaction Start Temperatures, and Minimum Rate Constants of the Reaction of Transition Metal Silicides with Hydrogen Chloride**

| silicide phase | reaction start temperature $T_{start}$/°C | minimum rate constant ln $k_{min}$ at $T_{start}$ | apparent activation energy absolute value/kJ mol$^{-1}$ | |
|---|---|---|---|---|
| | | | $T > T_{start}$ | $T < T_{start}$ |
| $Ni_2Si$ | 270 | −6.63 | 49.9 ± 1.8 | −35.7 ± 7.0 |
| $Cu_3Si$ | 310 | −6.29 | 69.8 ± 5.0 | −44.3 ± 2.4 |
| NiSi[a] | 313 | −4.07 | 88.1 ± 13.0 | −59.2 ± 5.1 |
| FeSi[a] | 355 | −4.42 | 41.6 ± 3.9 | −59.4 ± 0.6 |
| $Ni_3Si$ | 375 | −7.33 | 186.1 ± 9.2 | −19.6 ± 3.5 |
| $FeSi_2$[a] | 435 | −4.82 | 196.3 ± 22.1 | −137.6 ± 17.1 |
| $NiSi_2$[a] | 513 | −5.38 | 100.9 ± 15.1 | −115.8 ± 0.7 |

[a] Apparent activation energies have been published in ref 36.

rate, and it shows a narrow signal; the peak dropped after HCl was flushed out of the cell. Comparing $NiSi_2$, $Ni_2Si$, and $Ni_3Si$, the reaction time exceeds the residence time of hydrogen chloride in the cell.

**II. Solid-State Investigations.** To follow how chlorine interacts at the silicide surface, several studies of the surface region were performed. All nickel silicide phases (polished compact samples) were either directly treated with hydrogen chloride or were reacted under milder condition with hydrogen chloride by embedding the sample in $NiCl_2$ (having a water content lower than 1%), thus forming reaction layers with a thickness in the micrometer range and a composition different from that of the bulk. This process occurs within few minutes. Chlorine was present in all of these studies throughout the entire reaction layer.

Figure 4 shows the micrograph of a polished cross section of a NiSi sample treated with 0.8 bar hydrogen chloride at 410 °C for 8 min. The formed surface reaction layer consists of several layers with different chemical compositions. The gray tones depend on the nickel, silicon, and chlorine content. The distinctly separated layers indicate perpendicular nickel and silicon migration with respect to the surface plane. The drawing in Figure 4 shows the molar fraction of silicon as a function of depth and reveals an enrichment of nickel in the different reaction layers. According to XRD studies, the reaction layers on NiSi samples consist of $Ni_2Si$.

Previous XRD studies of the reaction of NiSi with hydrogen chloride or $NiCl_2$ for comparable time scales such as that of the surface studies (i.e., reactions were terminated before equilibrium) always gave $Ni_2Si$ (with more or less broadened or slightly shifted peaks) along with the unreacted NiSi phase.[13,30,31]

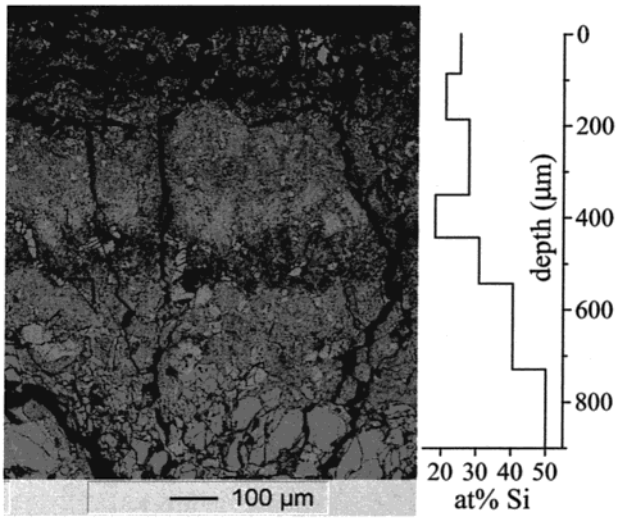


**Figure 4.** SEM micrograph of the reaction layer of a hydrochlorinated NiSi sample (left) and the silicon depth profile of the reaction layer (right).

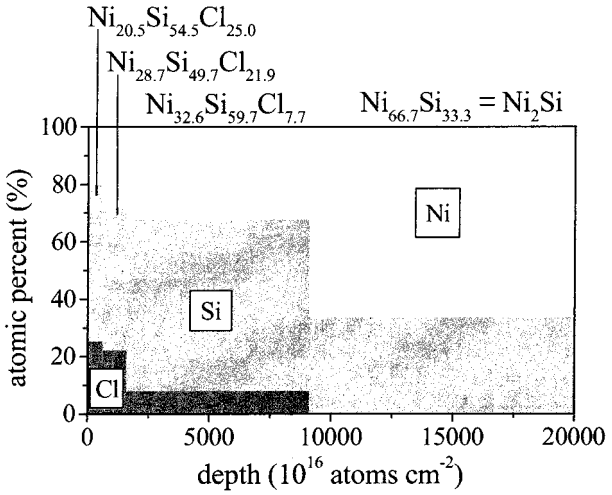


**Figure 5.** RBS profile of the surface region of a reaction layer.[36]

The RBS study reveals details of the uppermost surface region. Figure 5 proves the existence of a chlorine-rich surface layer and also confirms an enrichment of silicon near the surface.[23,24] The penetration depth of the helium atoms is too low to detect bulk NiSi, but a thick layer of $Ni_2Si$ is detected on which the chlorine- and silicon-rich layers are lying. The chlorine content in the $Ni_2Si$ layer was proven by SEM-EDX analysis of the same sample. The estimated thickness of the chlorine-containing layer is approximately 0.9 $\mu$m, which was estimated by assuming $10^{16}$ atoms cm$^{-2}$.

## Discussion

**I. Thermokinetic and Thermodynamic Studies. Apparent Activation Energies.** Negative activation energies are opposite to the general experience that rising temperature leads to an increase of the rate constant. In the literature, many examples of different origins are known in which this phenomena is explicitly discussed (e.g., OH addition to substituted ethenes,[37] hydrogen abstraction from aldehydes[38] and substituted aldehydes[39] by OH radicals, the silylene or germylene insertion into Si−H bonds[40] and Ge−H bonds,[41] respectively, and killing of mammalian cells and Drosophilia embryos[42] (and references therein for other biological systems)). The common explanation in all these articles is that the kinetically followed process

consists of a complex mechanism of at least two consecutive reaction steps. In numerous other articles, negative activation energies are shown in Arrhenius plots (e.g. silicon deposition by low-pressure MOCVD[43] or formation of formaldehyde in the oxidation of methanol on polycrystalline platinum[44]). Two examples of negative activation energies related to direct reactions of silicon are known: the formation of various silanes in direct synthesis on Si(100) surfaces[45] and a study of the reaction of cuprous chloride and silicon.[46]

To formulate a formalized kinetic model of an apparent negative activation energy, the reaction between hydrogen chloride and a silicide phase is thought of as a series of consecutive reactions. Below the reaction start temperature, hydrogen chloride is adsorbed on the surface and then incorporated into the silicide surface region in an exothermic reaction (formation of an intermediate), but gaseous products are not yet formed[30,31] or are formed only to a negligible extent. Here, the conversion of the intermediate into reaction products ($k_2$) is completely hindered but becomes possible predominantly above the reaction start temperature and results in a positive apparent activation energy.

In particular, the model of the negative apparent activation energy below the reaction start temperature consists of a fast adsorption of the gaseous compound (A (g)) and the reaction of the adsorbed molecules (A(ads)) with the underlying silicide phase to form a reaction intermediate I as the rate-limiting step, as shown in eq 5. For the sake of simplicity, only a single adsorbate case is considered. To include the dissociative chemisorption of hydrogen chloride, a model for the reaction path of the resulting chemically nonequivalent species would be required, which is not yet established.

$$\mathrm{A(g)} \rightleftarrows \mathrm{A(ads)} \xrightarrow{k_1} \mathrm{I\ (intermediate)} \xrightarrow{k_2} \text{solid} + \text{gaseous products} \quad (5)$$

Hence, the rate of formation of I is proportional to the hydrogen chloride coverage of the silicide surface (eq 6).

$$\frac{\mathrm{d[I]}}{\mathrm{d}t} = k_1 \Theta_{\mathrm{eq}} \quad (6)$$

The adsorption of the molecules is described by the Langmuir equation (eq 7).

$$\Theta_{\mathrm{eq}} = \frac{K_{\mathrm{a}} p_{\mathrm{eq}}}{1 + K_{\mathrm{a}} p_{\mathrm{eq}}} \quad (7)$$

$\Theta_{\mathrm{eq}}$ = coverage at equilibrium, $K_{\mathrm{a}}$ = the adsorption equilibrium constant, and $p_{\mathrm{eq}}$ = the equilibrium partial pressure of A(g), and by neglecting the denominator for low partial pressures ($K_{\mathrm{a}} p_{\mathrm{eq}} \ll 1$), eq 8 follows.

$$\Theta_{\mathrm{eq}} = K_{\mathrm{a}} p_{\mathrm{eq}} \quad (8)$$

By substitution of eq 8 into eq 6, eq 9 results:

$$\frac{\mathrm{d[I]}}{\mathrm{d}t} = k_1 K_{\mathrm{a}} p_{\mathrm{eq}} \quad (9)$$

The Arrhenius-type temperature dependence of the adsorption equilibrium constant $K_{\mathrm{a}}$ ($A_{\mathrm{a}}$ = the preexponential factor of adsorption, $\Delta_{\mathrm{a}}H$ = the adsorption enthalpy) and of the rate constant $k_1$ ($k_{1,0}$ = the preexponential factor, $E_{\mathrm{A}}$ = the activation energy) gives eq 10:

$$\frac{\mathrm{d[I]}}{\mathrm{d}t} = k_{1,0} A_{\mathrm{a}} p_{\mathrm{eq}} \mathrm{e}^{-(\Delta_{\mathrm{A}}H - E_{\mathrm{A}})/RT} \quad (10)$$

From eq 10 are the following results:

1. The reaction rate is proportional to the equilibrium pressure of the gaseous reactant.

2. The activation energy derived from an Arrhenius plot is an apparent activation energy, which consists of the adsorption enthalpy and the activation energy of the adsorption rate (according to the model): $E_{\mathrm{apparent}} = E_{\mathrm{a}} + \Delta_{\mathrm{a}}H$.

3. The relation between the exothermic adsorption enthalpy and the activation energy of the intermediate formation determines the slope of the apparent activation energy for the total process: $|\Delta_{\mathrm{a}}H| > E_{\mathrm{A}}$, which is a negative apparent activation energy for $T < T_{\mathrm{start}}$

In agreement with the model, it was found in a previous study[30,31] that a low hydrogen chloride partial pressure lowers the rate and increases the reaction start temperature. The reactions of two different NiSi to $NiCl_2$ molar ratios, (a) 1:0.2857 and (b) 1:0.5, were studied by isothermal DSC measurements.[30,31] The Avrami−Erofeyev equation was applied to calculate the rate constants, and the Arrhenius plot gave the same v-shaped pattern. Assuming that the same amount of moisture adhered to $NiCl_2$ because of the higher total amount of $NiCl_2$ in series (b), the hydrogen chloride partial pressure is higher than that for series (a). For both series, a reaction start temperature of 347 °C was found. For series (a) and (b), ln $k_{\mathrm{min}}$ values of −8.6 and −6.5 were found, respectively, compared to the corresponding 1 bar hydrogen chloride value of −4.07 and a characteristic temperature of 313 °C (Table 5). The obtained reaction start temperatures of 347 °C corresponds to the onset temperature when the chemical reaction between NiSi and $NiCl_2$ under the formation of gaseous products begins.[30,31]

Equation 10 shows, in accordance with the experimental results, that the reaction rate depends on the hydrogen chloride partial pressure. Therefore, this partial pressure must be kept constant for a series of measurementsto obtain comparable results.

The model of the apparent negative activation energy is consistent with the results in Figure 1 that show that the measured heat of reaction increases with increasing temperature for all of the studied silicide phases. Although the heat of adsorption should decrease with rising temperature, the incorporation of hydrogen chloride (intermediate formation) becomes more important. Therefore, the thermal signal below the reaction start temperature is the sum of the exothermic hydrogen chloride chemisorption and the exothermic chlorine incorporation into the silicide surface region.

**Reaction Start Temperature as a Thermodynamic Parameter.** In Figure 6, the reaction start temperatures of nickel silicides are plotted as a function of the molar fraction of silicon. The plot shows that the obtained curve corresponds to the standard formation enthalpies of the silicides at 298.15 K,[47] to the heat of mixing of liquid nickel and liquid silicon (values shown here are at 1800 K[47]), and to the curve for the heat of chlorine dissolution in nickel silicides.[32] This general agreement leads to the conclusion that the enthalpy of chlorine intake into nickel silicides is proportional to the strength of interaction between nickel and silicon in the solid or liquid phase. Furthermore, these curves are in agreement with the reaction start temperatures; therefore, the reaction start temperature is considered to be a thermodynamically determined parameter.

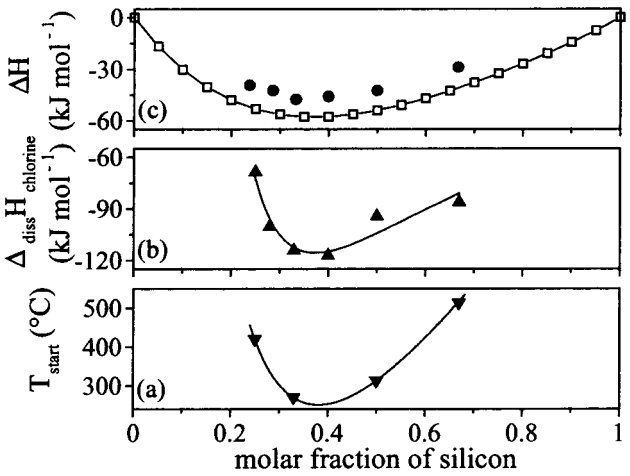


**Figure 6.** Correlation of the reaction start temperature for various nickel silicide phases (a) to the enthalpy of chlorine dissolution in nickel silicide phase (b) and to thermodynamic functions of the nickel−silicon system (c) (● represents the standard enthalpy of formation of nickel silicides at 298.15 K,[47] and □ represents the mixing enthalpy of nickel and silicon at 1800 K[47]).

The question remains of what parameters can be used to discuss the differences in the reactivity between various transition metal silicides or between various metal-to-silicon ratios of one metal. Band structure calculations of transition metal silicides show the presence of mainly covalent bonds and minor ionic contributions for the late 3d transition metals[48−53] and a higher ionic contribution for $Cu_3Si$,[54] but these calculations are not able to reflect trends in the reactivity of transition metal silicide phases. Rather, enthalpies and excess entropies of mixing of silicon and transition metals more suitably reflect this phenomenon. In the metal row from Mn to Ni, the enthalpy and excess entropy of mixing increase, but they decrease for Cu: $\Delta_{mix}H_{Ni-Si} = (-56.0 \pm 2.1)$ kJ mol$^{-1}$ at $x_{Si} = 0.39$, $\Delta_{mix}H_{Cu-Si} = (-14.0 \pm 0.6)$ kJ mol$^{-1}$ at $x_{Si} = 0.25$, $\Delta_{mix}S(\text{excess})_{Ni-Si} = (-17 \pm 3)$ J K$^{-1}$ mol$^{-1}$ at $x_{Si} = 0.38$, $\Delta_{mix}S(\text{excess})_{Cu-Si} = (-4 \pm 0.5)$ J K$^{-1}$ mol$^{-1}$ at $x_{Si} = 0.20$.[55,56] The large negative excess entropy of mixing arises from the electron contribution by transfer of silicon valence electrons to fill the metal 3d shell. The atomic interaction between 3d metals and silicon is stronger as the 3d shell fills with electrons. The decrease in the excess enthalpies and entropies of mixing from nickel to copper is a result of the completely filled d shell ($3d^{10}$-$4s^1$) of copper.[55,56] The thermodynamic approach is able to explain similar chemical properties of chlorine-containing iron, cobalt, and nickel silicide phases in the hydrodechlorination reaction and the comparable chlorine contents as well as the exception of copper silicide phases.

**Kinetics and Apparent Activation Energies.** As expected, the largest minimum rate constants in Figure 7 go along with a low positive apparent activation energy in Figure 8.

Reaction start temperatures (Figure 7) and positive apparent activation energies (Figure 8) show a comparable dependence on the molar fraction of silicon. A low reaction start temperature and hence strong metal−silicon interactions and a high chlorine solubility correspond to a low apparent activation energy, indicating that chlorine intake is directly related to the reactivity of the silicide phases. Over the whole composition range, the thermodynamic parameter $T_{start}$ and the minimum rate constant are inversely dependent on the molar fraction of silicon (Figure 7). A low rate is observed for low and high silicon content, and the maximum seems to be an optimum value between two opposite tendencies. To explain the kinetic behavior, we propose

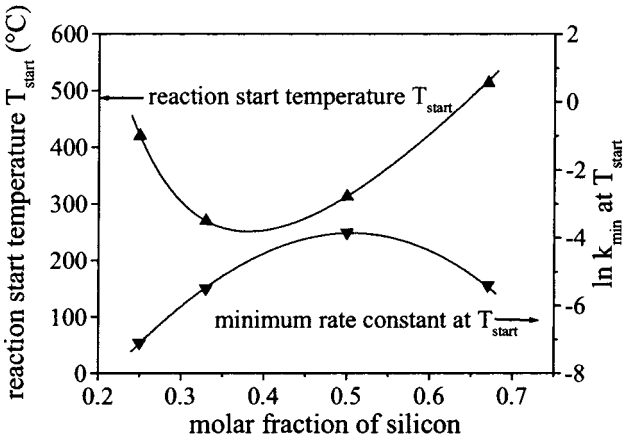


**Figure 7.** Reaction start temperatures and minimum rate constants for the reaction of the various nickel silicide phases with hydrogen chloride as a function of the molar fraction of silicon.

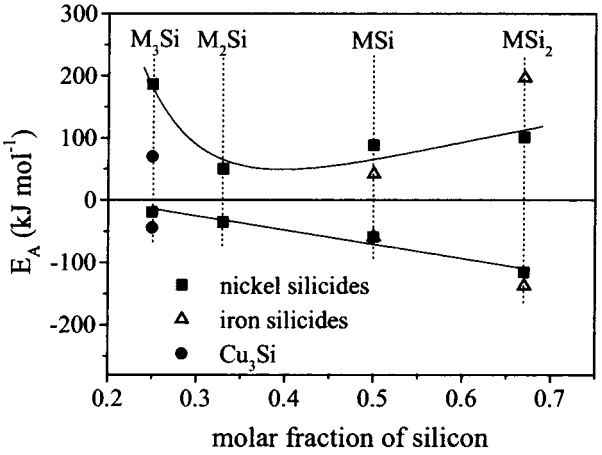


**Figure 8.** Apparent activation energies for the reaction of various silicide phases with hydrogen chloride as a function of the molar fraction of silicon.

to divide the silicide surface/reaction region into a number of chlorine adsorption sites, which is proportional to the molar fraction of the metal, and into a number of silicon reaction sites, which is proportional to the molar fraction of silicon. Disilicides have a low number of chlorine adsorption sites and a high number of silicon reaction sites, and hydrogen chlorine bound to the surface is readily converted into silanes and hydrogen. As a result, the heat-flow signal is quite narrow, and the reaction rate is high. Because of its high metal content, the $M_3Si$ phase allows high chlorine coverage, but the reaction proceeds at a low rate because of the low number of silicon reaction sites. Hence, a broadened heat-flow signal is observed. The "chlorine absorption site" and "silicon reaction site" do not necessarily imply that all of these sites are directly located on the surface or that these sites can be considered to be surface species. It also should not be concluded that chlorine is bonded to nickel. Rather, the metal should be considered to be an intermediary that transfers chlorine to silicon according to a general mechanism (Scheme 1) suggested by Lewis et al.[20]

The linear dependence of the negative activation energies on the molar fraction of silicon is difficult to explain. It seems that a high metal content lowers the activation barrier of chlorine incorporation because of a higher number of chlorine adsorption sites. High nickel mobility may also support the incorporation of chlorine into the silicide phases (see later discussion). As in the case of the positive apparent activation energies, no dependence on the silicide phases crystal structure exists.

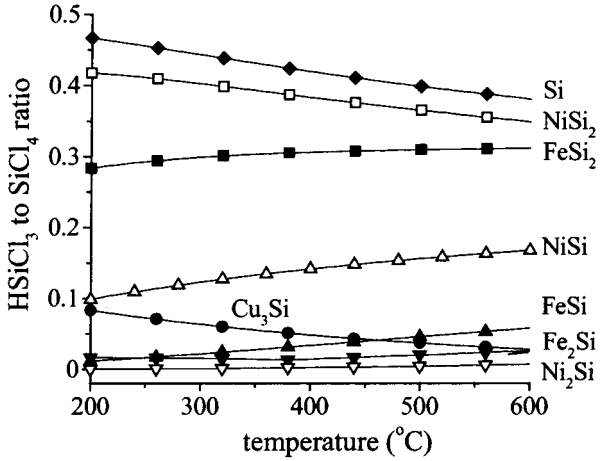


**Figure 9.** Trichlorosilane-to-silicon tetrachloride ratio calculated for various iron, nickel, and copper silicide phases.

**SCHEME 1. General Mechanism of the Direct Reaction of Silicon and Hydrogen Chloride According to Lewis et al.[24]**

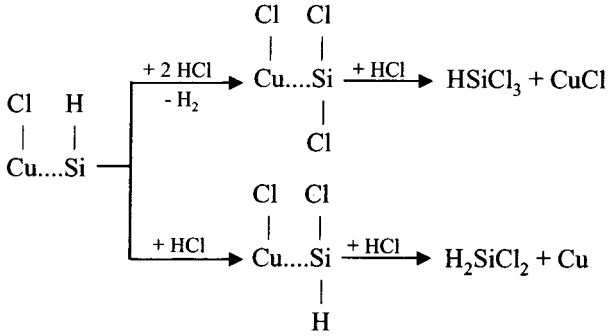


**Reaction Products.** In the previous sections, the formed gaseous products were neglected, but here, the product distribution of formed silanes is discussed on the basis of thermodynamic considerations. The product gas-phase composition was thermodynamically calculated for the reactions of hydrogen chloride and various silicide phases in a molar ratio of 1:100, respectively. The obtained trichlorosilane-to-silicon tetrachloride ratio is plotted as a function of temperature in Figure 9.

Pure silicon gives the highest trichlorosilane yield, followed by the disilicides of nickel and iron. Generally, with increasing metal content, the trichlorosilane yield decreases, and $Ni_3Si$, which is not indicated in the diagram, gives no appreciable amount of trichlorsilane (ratios at 200 and 600 °C are $5 \times 10^{-5}$ and 0.0015, respectively). Having a high number of chlorine adsorption sites favors silicon tetrachloride or, generally, a high chlorine content in the gaseous product phase. Furthermore, iron silicides always produce more silicon tetrachloride than do nickel silicide phases of the same metal-to-silicon ratio. Therefore, the chlorine content of the product silanes also correlates with the metal−chlorine bond strength of Fe > Ni > Cu (Table 3). Copper is a remarkable exception in two cases: (i) despite its high metal content, it gives a high trichlorosilane yield (Figure 9) and (ii) it is the only metal that also produces dichlorosilane in a reasonable yield (here calculated and experimentally proven for copper−silicon mixtures in ref 57).

**Direct Synthesis Promoters.** On the basis of the presented results, some general principles about structural promoters in direct reactions of silicon can be derived. According to Lewis et al., structural promoters cause a change in chemical composition in the solid phases.[20,24]

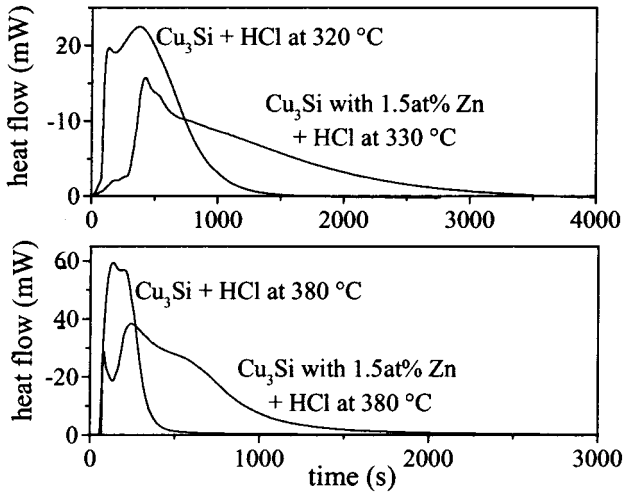


**Figure 10.** Heat-flow curves of the reaction of $Cu_3Si$ and $Cu_3Si$ + 1.5 at. % Zn with hydrogen chloride at various temperatures. Because of the structures in the curves of $Cu_3Si$ + 1.5 at. % Zn, only the tails of the curves were fitted by the Avrami−Erofeyev equation.

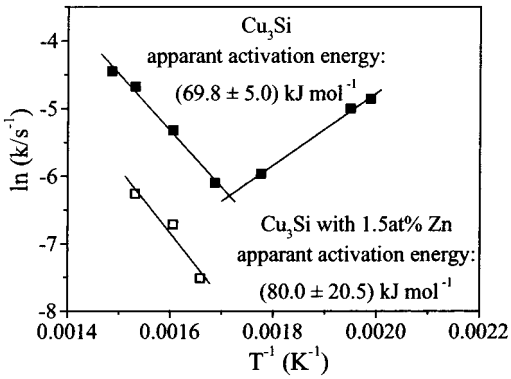


**Figure 11.** Arrhenius plot of the reactions of $Cu_3Si$ and $Cu_3Si$ + 1.5 at. % Zn with hydrogen chloride.

(i) To increase the reaction rate of metal-rich silicide phases, the number of silicon reaction sites has to be increased by a higher diffusion rate of silicon to the surface. Alternatively, chlorine transfer from the chlorine adsorption sites to the silicon reaction sites can be enhanced. We studied the reaction of a $Cu_3Si$ alloyed with 1.5 at. % Zn with hydrogen chloride in the same manner as that described above. As can be seen from Figure 10, zinc addition causes a stronger interaction with hydrogen chlorine. We have found that the rate is decreased dramatically with a parallel shift in the rate and with a conserved apparent activation energy (Figure 11). The optimum amount of a zinc promoter is around 0.4 at. % Zn.[24] From the parallel shift, we conclude that an excess of zinc (more than the optimum) decreases the reaction rate by lowering silicon diffusion to the surface without changing the reaction mechanism.

(ii) To decrease the reaction start temperature of silicon-rich silicide phases, a small amount of a metal could be introduced that strongly interacts with silicon and therefore enhances the ability of chlorine intake. Side products may play a role here. Furthermore, silicide phases having a high silicon content have a smaller number of chlorine adsorption sites compared to their high number of silicon reaction sites. A metal chloride (or its pure metal, as a precursor) that sticks on the surface and hence causes a higher chlorine content on the surface than the initial silicide phase would be able to form may be introduced. Ideally, the metal chloride should give its chlorine easily to the silicon

reaction sites, and the metal chloride should easily be regenerated by the hydrogen chloride from the gas phase.

Introducing additional compounds may also cause synergistic effects between the reaction start temperature and reaction kinetics and may explain why different promoters show unexpected behaviors in different concentration ranges and in mixtures with other promoters.[7]

## Summary

The reactivity of transition metal silicides can be described by thermodynamic and kinetic parameters that are clearly separated from each other:

(1) The characteristic temperature correlates to the silicide phases thermodynamic functions as standard enthalpies of formation, mixing enthalpies of the liquid elements, and enthalpies of chlorine dissolution. The characteristic temperature is an expression of metal−silicon interactions with respect to the ability to incorporate chlorine into the lattice structure. As the chlorine intake increases, the characteristic temperature decreases. The silicide phase crystal structures do not seem to play a role in reactivity.

(2) Chlorine adsorption sites and silicon reaction sites are introduced to discuss the minimum rate constants as a function of the silicide phase composition and to explain the shape of the calorimetric signals. Reaction start temperatures, positive apparent activation energies, and minimum rate constants show the same dependence on the molar fraction of silicon. Therefore, the presence of chlorine in the silicides is the necessary condition for their reactivity. The negative apparent activation energies, increasing linearly with silicon content, are attributed to hydrogen chloride chemisorption and chlorine intake into silicide phases below the reaction start temperature.

(3) A high metal content of the reacting silicide phase favors silicon tetrachloride formation. Silicides of metals known to form a strong metal−chlorine bond yield more silicon tetrachloride than do metal silicides whose metal forms a metal−chlorine bond of lower strength. Copper is an exception and forms dichlorosilane.

(4) A high metal concentration correlates to strong hydrogen chloride chemisorption (Figure 3, chlorine adsorption sites) and to a high silicon tetrachloride yield, although metal chloride formation was never observed, which points to the role of the metal as a transmitter of chlorine to silicon in a spill-over process. This result is consistent with Lewis' general mechanism of direct reaction[20] in which chlorine transfer from metal to silicon is the key step of silylene species formation (Scheme 1).

**II. Solid-State Investigations.** To introduce the following discussion, a brief review of diffusion phenomena in the nickel−silicon system is necessary. By the reaction of thin films of nickel and silicon at around 400 °C, $Ni_2Si$ is growing as the first phase by a diffusion mechanism. If all nickel is consumed in the formation of $Ni_2Si$, NiSi, which is formed by diffusion, appears at around 500 °C. Finally, $NiSi_2$ is formed by nucleation around 800 °C.[58,59] Because of a nucleation hindrance, $Ni_3Si_2$ is formed only when the temperature is equal to or higher than 600 °C at the interface in the $Ni_2Si$/NiSi diffusion couple.[60] An interesting phase formation pathway was found in the case of $Ni_2Si$ and NiSi. NiSi is found to grow between a Si/$Ni_2Si$ interface via decomposition of $Ni_2Si$ into NiSi and Ni. The nickel atoms move backward to the silicon interface and react there with silicon atoms, forming NiSi.[61] The reaction of nickel with silicon was determined to be the rate-limiting step, not the nickel diffusion in NiSi. In all nickel silicide phases, nickel

**SCHEME 2. Formation of a $Ni_2Si$ Layer on NiSi as a Result of Nickel Diffusion.**

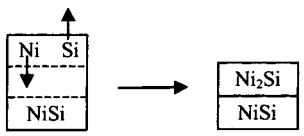


was found to be the mobile atom, and the silicon atom mobility is about 10% of that of the nickel atoms.[60] In $Ni_2Si$, the majority of the atoms constitute a network where vacancies can easily migrate. In the case of NiSi, the nickel and silicon atoms are located in geometrically different sites, and nickel migrates via vacancies in the nickel sublattice. In $NiSi_2$, the nickel motion is assumed to proceed via the empty cube centers of the unit cell. To increase the relative diffusion rate of silicon, a larger activation energy is required compared to that of the mobilization of nickel atoms.[59,62]

On the basis of these results, the phase formation sequence for the nickel silicide phases $Ni_2Si$, NiSi, and $NiSi_2$ can be described by the following equation where $Ni_3Si_2$ formation is omitted:

$$NiSi_2 \underset{-Ni}{\overset{+Ni}{\rightleftharpoons}} 2NiSi \underset{-Ni}{\overset{+Ni}{\rightleftharpoons}} 2Ni_2Si \qquad (11)$$

**SEM-EDX Study.** The formation of a $Ni_2Si$ reaction layer on bulk NiSi as found by the SEM-EDX study (Figure 4) is easily explained as a diffusion phenomenon (eqs 12 and 13).

$$NiSi + 4HCl \rightarrow Ni + SiCl_4 + 2H_2 \qquad (12)$$

$$NiSi + Ni \rightarrow Ni_2Si \qquad (13)$$

Silicon is removed from the silicide surface by reacting with hydrogen chloride. The excess nickel atoms diffuse into the underlying NiSi layer to form $Ni_2Si$ (Scheme 2).

According to this simple model, chlorine incorporated into the silicide bulk phase does not seem to play an important role. Chlorine becomes the only matter of importance to the question of whether $NiCl_2$ is found as a reaction product or not. The absence of $NiCl_2$ can be explained by the following thermodynamic consideration (eq 14). Metal chloride formation does not occur if the metal chloride can be reduced by silicon (or another silicide phase) under the formation of a (or another) silicide phase. As a rule of thumb, the free enthalpy of chloride formation must be less than $-320$ kJ mol$^{-1}$, as in the case of iron, cobalt, nickel, and copper (exact values for any metal and temperature can be calculated).[36]

$$4/xMCl_x + (4y/x + 1)Si \rightarrow 4/xMSi_y + SiCl_4(g) \qquad (14)$$

When the reaction conditions are mild, silicon is always present at or near the surface. The possibly formed nickel−chlorine bonds can be reduced by silicon, and chlorine is transferred from nickel to silicon by the same process. Hence, the absence or presence of $NiCl_2$ is a clear indication that the reaction conditions are dominated by thermodynamics or kinetics, respectively. If silicon is removed under aggressive reaction conditions, $NiCl_2$ is immediately formed despite the thermodynamic capability of silicon (or a present silicide phase) to reduce $NiCl_2$ according to eq 14. The lower free enthalpy of formation of copper chloride explains the higher activity of copper chloride at low temperatures compared to that of the chlorides of iron, cobalt, and nickel.

**SCHEME 3. Formation of a Chlorine-Containing Reaction Layer.**

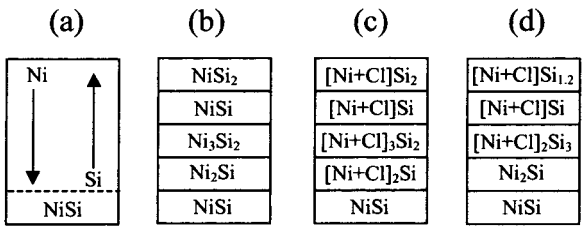


(a) Hydrogen-chloride induced motion of nickel and silicon atoms yields the idealized silicide phase sequence in (b). For the sake of simplicity, stoichiometric considerations between the layers are omitted, and a uniform layer thickness is drawn. (c) Expected layer composition if nickel sites are occupied by chlorine. (d) Results from the RBS study.

**RBS Study.** A more detailed understanding of the reaction surface layer and the role of chlorine is obtained by Rutherford backscattering studies on hydrochlorinated NiSi samples (Figure 5). To explain the formed layers of different compositions, we refer to eq 11. Applying this equation, the phase sequence as shown in Scheme 3b should be obtained. As seen from Figure 5, a high chlorine content corresponds to a low nickel content and vice versa. The conclusion is that chlorine displaces nickel by occupation of nickel sites. Occupancy of nickel sites by chlorine forces nickel atoms to move into the bulk, and silicon atoms diffuse to the surface by counter diffusion. Recalculating the nickel content as nickel = [nickel + chlorine] and the nickel-to-silicon ratio, a layer sequence is obtained that matches the composition of the layer (Scheme 3c and d). It should be noted that the diffusion model describes a system of constant mass, and the RBS study is taken at an early stage of the reaction in which silicon is already removed from the bulk.

The assumption of the occupation of nickel sites by chlorine is indirectly supported by in situ XRD studies of the reaction of NiSi and $NiCl_2$.[13] It was found that the silicide phase degradation always proceeds through ordered structures, either through $Ni_2Si$ at 410 °C or through an unknown intermediate ordered structure at 390 °C. Amorphization was never observed in any of our studies, but numerous presumably kinetically determined ordered structures were identified.[30]

Some questions arising from the presented model should be discussed here. The formation of silicon tetrachloride is the thermodynamic driving force of the hydochlorination reaction. Chlorine incorporation into the lattice can be thought of as a series of states in which a silicon atom makes a transition from a lattice atom to a silicon tetrachloride molecule. Therefore, chlorine incorporation is thermodynamically driven. The fact that chlorine is diluted in a silicide phase can be understood as an analogue to oxygen solubility in titanium or zirconium[63] or to the oxidation of metals or alloys by diluted oxygen.[2]

On the microscopic level, chlorine incorporation is assumed to proceed by the displacement of nickel atoms, followed by the occupation of nickel atoms sites with chlorine. Nickel atoms are forced to move toward the bulk, but silicon atoms seem to diffuse to the surface. The high mobility of silicon might be a combination of (i) silicon diffusion along the chlorine concentration gradient using defects created by chlorine and nickel motion; and (ii) fast diffusion of nickel atoms into the bulk and exposing the less mobile silicon atoms to the surface. This result might explain that the reaction of nickel silicides with hydrogen chloride is a very selective reaction. Not all silicon atoms seem to be immediately attacked by hydrogen chloride or incorporated chlorine so that silicon atoms remain, which constitutes an ordered structure of the reaction layer. The reaction layer itself consists of various layers having different compositions. The diffusion of nickel, silicon, and chlorine can explain the observed sublayer sequence.

**TABLE 6: Adiabadic Electron Affinities of Gaseous Silylenes**

| species | electron affinity/eV | ref | species | electron affinity/eV | ref |
|---|---|---|---|---|---|
| $SiH_2$ | $1.124 \pm 0.020^a$ | 65 | $SiCl_2$ | $0.64; 0.90^a$ | 74 |
| $SiH_2$ | $1.2^a$ | 66 | $SiCl_2$ | $0.79; 1.25^b$ | 75 |
| $SiH_2$ | $1.003^b$ | 67 | $SiCl_2$ | $1.26; 1.50^c$ | 76 |
| $SiH_2$ | $1.37; 1.00^c$ | 68 | $HSiCH_3$ | $-0.018^b$ | 69 |
| $SiH_2$ | $1.029^b$ | 69 | $Si(CH_3)_2$ | $-0.064^b$ | 69 |
| $SiH_2$ | $1.17^b$ | 70 | | | |
| $SiH_2$ | $1.12^a$ | 71 | $CH_3$ | $0.08 \pm 0.03^a$ | 77 |
| $SiH_2$ | $1.16^b$ | 72 | $CH_3$ | $0.07^b$ | 78 |
| $SiH_2$ | $1.03; 1.08; 1.20^c$ | 73 | | | |

[a] Experimental. [b] Calculated. [c] Calculated by various models.

The main consequence of the formed reaction layer is a local separation of the proceeding reaction steps. The sites where the dissociative chemisorption of hydrogen chloride occurs, where chlorine and hydrogen are attached to silicon, yielding silylenoide surface species, and where surface species react to form product molecules are not identical. Away from the surface, silicon atoms at the interface between the reaction layer and the unreacted silicide phase are removed from the pure silicide phase and forced into the reaction layer. The mechanism of this interface reaction is unclear; silicon might be removed from the pure silicide phase by a direct reaction with chlorine or might be loosened from the pure phase by reacting with the backward-diffusing nickel atoms.

Results from the gas-phase silicidation of nickel by a $SiCl_4/H_2$ gas mixture point to an associated mobility of silicon−chlorine clusters within a nickel matrix.[13]

**III. Suggestion of a Model for the Reactive Surface Layers.** At the present point of research, the bonding character of chlorine incorporated into the silicide phases is yet unknown. But it had been shown that the chemical properties of chlorine-containing silicide phases are different from the chemical properties of pure silicide phases. Furthermore, the chlorine−silicon interaction in the chlorine-containing phases is much stronger than the metal−silicon interactions (thermal decomposition). Therefore, it is at least reasonable to assume that chlorine intake changes the electronic structure with respect to that of the initial silicide phase.

In the following section, the role of the chlorine-containing reaction layer is discussed using the model of electronegativity equalization. This model says that different species have different electronic chemical potentials and that at equilibrium electrons flow from one species to another to equalize the chemical potential.[64] To determine the stability of silylenoids on the silicide surface, we consider the adiabatic electron affinities of gaseous silylenes and the work function of the surface reaction layer. As seen from Table 6, electropositive and electronegative silylenes are known.

$$SiCl_2 > (HSiCl) > SiH_2 > CH_3 > (CH_3SiCl) > HSiCH_3 > Si(CH_3)_2 \quad (15)$$

The sequence in eq 15 represents the known adiabatic electron affinities of gaseous silylenes. The electronegative character increases with the substituents and their number bound to silicon as Cl > H > $CH_3$. For HSiCl and $CH_3SiCl$, there is no data available, but the substituents have been ordered according to their character. The work functions of chlorine-containing

silicides are not known. On the basis of the concept of electronegativity equalization, a higher electron density is necessary to stabilize the electronegative $SiCl_2$, whereas $HSiCH_3$ is already stabilized by the lower electron density of the reaction layer.

Instead of the unknown work functions of the chlorine-containing silicide phases, we refer to the observed steady-state product distributions in the direct synthesis and hydrochlorination (Tables 1 and 2). It is assumed that these products are formed by the reaction of a silylenoide species with either hydrogen chloride or methyl chloride.[20] From the product distributions (Tables 1 and 2), it can be concluded that the copper-based, chlorine-containing reaction layers have a lower electron density than do nickel- or iron-based reaction layers, which is in accordance with the lower interaction of copper and silicon compared to that of iron, cobalt, or nickel and silicon.[55,56] According to the product distributions in Tables 1 and 2, reaction layers or chlorine-containing silicide phases formed by reaction with hydrogen chloride or a silicon tetrachloride/ hydrogen mixture prefer more electronegative silylenoide species than does the same chlorine-containing silicide phase formed in the reaction with methyl chloride. Here, the difference is the result of the acid−base strengths of methyl chloride and hydrogen chloride. The reactivity seems not to depend on the possible maximum intake of chlorine but rather on the amount of accessible chlorine. Hence, a silicide phase can exhibit a wide range of reactivity, and its reactivity can be dramatically changed by the addition of small amounts of promoters.

On the basis of these considerations, a model of the induction period of the direct synthesis is proposed. At the first exposure of a copper silicide sample, methyl chloride decomposes on the surface into carbon, hydrogen, and chlorine. Methane, hydrogen, and hydrocarbons are formed, and chlorine incorporation starts. Because of the low chlorine content of the copper silicide surface layer, the electron level is quite low. Therefore, the preferred electropositive silylenoids $HSiCH_3$ and $Si(CH_3)_2$ are stabilized. By inserting methyl chloride molecules into these silylenoids, $(CH_3)_2SiHCl$ and $(CH_3)_3SiCl$ are formed. Over the time of the reaction, chlorine intake proceeds and the surface region incorporates chlorine as long as the steady-state chlorine concentration, according to the steady-state methyl chloride partial pressure, is not reached. When the steady-state chlorine uptake is reached, the higher electron level is higher than that in the previous period. Hence, more electronegative silylenoids, like $CH_3SiCl$, can be stabilized, and dichlorodimethylsilane is formed by inserting methyl chloride molecules. In combination with methyl chloride, copper-based solid phases are not able to stabilize $SiCl_2$ silylenoides. Generally, this model always implies the formation of silanes with a higher hydrogen or methyl content than that under later steady-state conditions.

Temperature and surface chlorine concentration have additional effects on the product distribution. In hydrochlorination, silicon tetrachloride is the thermodynamically stable product and what is preferably formed at high temperatures. Trichlorosilane is considered to be a kinetically preferred product at low temperatures. It is assumed that electropositive hydrogen-rich surface species (silylenoides) are more stable at low temperatures.[36] Furthermore, the increasing metal content of the solid phase (e.g., by silicon depletion) leads to an increase of the silicon tetrachloride yield (Figure 9). Hence, a higher number of chlorine adsorption sites are formed, and the chlorine concentration at the surface increases remarkably.[36]

Our model explains the differences in product distribution through changes in the electronic structure of the reaction layer and the gradual differences in the reactivity between various metals on the basis of a correlation of mixing enthalpies and entropies of transition metal−silicon systems. From the results in Tables 1 and 2, one might conclude that the product distribution of direct synthesis and the hydrochlorination reaction follows the polarity of metal−silicon bonds. Ranging from late transition metals, which form mainly covalent silicides,[48−53] to ionic magnesium and calcium silicides, chlorine is attached to the positively charged metal constituent. The remaining substituents (either hydrogen or a methyl group) are bound to the negatively charged silicon. We do not follow this consideration, which is similar to Voorhoeve's model,[79] because the presence of chlorine changes the bonding state in the silicide phases.

Our model can be understood as an extension of Roewer's model of the hydrodechlorination reaction,[10] which introduces an electron-transfer process from an adsorbed silicon tetrachloride molecule to a silicide surface under the formation of a silylenoide surface species.

**IV. Some Comments about the Role of Hydrogen.** We have to emphasize that the role of hydrogen is still unknown in the direct reactions and in the hydrodechlorination reaction as well. All analytical methods employed failed to detect hydrogen in the solid phases. Therefore, hydrogen is not included in our consideration.

But, the silicon−hydrogen system exhibits a large variety of surface chemistry on crystalline[80] and on porous[81] silicon. Certainly, hydrogen plays an important role in direct reactions, but as bonded hydrogen in hydrogen chloride or trichlorosilane rather than as molecular hydrogen. Few examples should underline this result. In the hydrodechlorination reaction of silicon tetrachloride, it was found that only a sufficient pulse of hydrogen chloride reactivates an inactive catalyst, whereas molecular hydrogen is inactive.[9,10] Hydrogen chloride,[5] chlorine,[5] and trichlorosilane[29] were found to activate the copper−silicon mass in direct synthesis by forming silicon−chlorine surface species. It seems that a certain hydrogen concentration bound to the surface is required to start and to maintain the reaction propagation. In the direct synthesis of phenylchlorosilane using phenyl chloride and a copper−silicon mixture, an addition of hydrogen chloride increased the rate of trichlorphenylsilane and diphenyldi- chlorosilane, although hydrogen chloride is formally not involved.[82,83]

## Conclusion

The present study gives a comprehensive and quantitative view of the chemical reactivity of intermetallic compounds, particularly for the reactions of transition metal silicides and hydrogen chloride. Macroscopic and microscopic approaches are presented and unified in a model of chlorine dissolution in silicide phases.

On the basis of calorimetric measurements, reaction start temperatures, rate constants, and apparent activation energies were determined. Reaction start temperatures and positive apparent activation energies are related to the model of chlorine solubility and can be understood as expressions of the interactions between metal and silicon in the silicide phases. High chlorine solubility is correlated to a low reaction start temperature, to a low positive apparent activation energy, and to a high reaction rate. Negative apparent activation energies are considered to describe the chemisorption of hydrogen chloride and the incorporation of chlorine into the surface region of the silicide phases at temperatures too low to form gaseous products. Solid-state studies proved the formation of a chlorine-containing reaction layer by exposing the silicide phases to hydrogen

chloride. The formation, renewal, and microscopic structure of such a layer can be explained by diffusion.

The chlorine-containing reaction layer acts as a transmitter between the pure underlying silicide phase and the gas phase and is attributed to a local separation of elemental reaction steps. The level of chlorine intake adjusts the electronic properties of the reaction layer and determines what silylenoide surface species are stabilized.

Primarily, the reactivity of the silicon atoms in the silicide phases is determined by the metal. The strength of metal−silicon interactions correlates to the chlorine intake ability. Thermodynamic parameters such as enthalpies of mixing or formation are found to be more useful to explain metal−silicon interactions rather than band structures of silicide phases. As a second parameter, the acid−base strength of the reaction gas phase determines the chlorine intake as well. Different product distributions between reactions with methyl chloride or hydrogen chloride can be explained in this manner. Furthermore, the change in reactivity from metal-rich to silicon-rich silicide phases can be explained only when the existence of chlorine adsorption sites (related to the metal content) and silicon reaction sites (related to the silicon content) is assumed. The essential step here is a spill-over process where chlorine is transferred from chlorine adsorption sites to silicon reaction sites.

Yet unclear is how hydrogen is involved in the reaction mechanism of chlorosilane formation.

**Acknowledgment.** We gratefully acknowledge Dr. Kenrick M. Lewis, Osi Specialties, Crompton Corporation, Tarrytown, NY, and Professor Gerhard Roewer, Freiberg University, for fruitful discussions. We thank Dr. S. Roosendaal and Dr. A. J. Vredenberg, Department of Atomic and Interface Physics, State University Utrecht, The Netherlands, for RBS investigations and Dr. N. Mora-Diez, Department of Chemistry, Dalhousie University, Halifax, Nova Scotia, Canada, for manuscripts of submitted papers. J.A. thanks the Alexander von Humboldt Foundation for funding provided by a Feodor Lynen Fellowship.

## References and Notes

(1) Sinfelt, J. H. *Prog. Solid State Chem.* **1975**, *10*, 55.
(2) Schmalzried, H. *Chemical Kinetics of Solids*; VCH: Weinheim, Germany, 1995.
(3) Voorhoeve, R. J. H. *Organohalosilanes: Precursors to Silicones*; Elsevier: Amsterdam, 1967.
(4) Bazant, V. *Pure Appl. Chem.* **1969**, *19*, 473.
(5) Turetskaya, R. A.; Andrianov, K. A.; Trofimova, I. V.; Chernyshev, E. A. *Russ. Chem. Rev. (Engl. Transl.)* **1975**, *44*, 212.
(6) Clarke, M. P. *J. Organomet. Chem.* **1989**, *376*, 165.
(7) *Catalyzed Direct Reactions of Silicon;* Lewis, K. M., Rethwisch, D. G., Eds.; Studies in Organic Chemistry Series 49; Elsevier: Amsterdam, 1993.
(8) Bohmhammel, K.; Roewer, G.; Walter, H. *J. Chem. Soc., Faraday Trans.* **1995**, *91*, 3879.
(9) Walter, H. Ph.D. Thesis, Freiberg University of Mining and Technology, Freiberg, Germany, 1995.
(10) Walter, H.; Roewer, G.; Bohmhammel, K. *J. Chem. Soc., Faraday Trans.* **1996**, *92*, 4605.
(11) Over, H.; Kim, Y. D.; Seitsonen, A. P.; Wendt, S.; Lundgren, E.; Schmid, M.; Varga, P.; Morgante, A.; Ertl, G. **2000**, *287*, 1474.
(12) Frank, T. C.; Kester, K. B.; Falconer, J. L. *J. Catal.* **1985**, *95*, 396.
(13) Acker, J.; Röver, I.; Otto, R.; Roewer, G.; Bohmhammel, K. *Solid State Ionics* **2001**, *141*−*142*, 583.
(14) Mulla, I. S.; Choube, A. C.; Dongare, M. K.; Sinha, A. P. B. *Indian J. Chem., Sect. A* **1988**, *27*, 756.
(15) Acker, J.; Bohmhammel, K.; Henneberg, E.; Irmer, G.; Röver, I.; Roewer, G. *Adv. Mater. (Weinheim, Ger.)* **2000**, *12*, 1605.
(16) Barin, I. *Thermochemical Data of Pure Substances*; VCH Verlags Gesellschaft: Weinheim, Germany, 1993; Parts I and II.
(17) Kautsky, H.; Pfleger, H. *Z. Allg. Anorg. Chem.* **1958**, *295*, 206.
(18) Weiss, A.; Beil G.; Meyer, H. *Z. Naturforsch., B: Chem. Sci.* **1980**, *35*, 25.
(19) Yamanaka, S.; Matsuura, H.; Ishikawa, M. *Mater. Res. Bull.* **1996**, *31*, 307.
(20) Lewis, K. M.; McLeod, D.; Kanner, B.; Falconer, J. L.; Frank, T. C. In *Catalyzed Direct Reactions of Silicon;* Lewis, K. M., Rethwisch, D. G., Eds.; Studies in Organic Chemistry Series 49; Elsevier: Amsterdam, 1993; p 333.
(21) Clarke, M. P.; Davidson, I. M. T. *J. Organomet. Chem.* **1991**, *408*, 149.
(22) Okamoto, M.; Onodera, S.; Okano, T.; Suzuki, E.; Ono, Y. *J. Organomet. Chem.* **1997**, *531*, 67.
(23) Frank, T. C.; Falconer, J. L. *Appl. Surf. Sci.* **1982**, *14*, 359.
(24) Lewis, K. M.; McLeod, D.; Kanner, B. In *Catalysis 1987: Studies in Surface Science and Catalysis*; Ward, J. W., Ed.; Elsevier: Amsterdam, 1988; Vol 38, p 415.
(25) Banholzer, W. F.; Burrell, M. C. *Surf. Sci.* **1986**, *176*, 125.
(26) Banholzer, W. F.; Burrell, M. C. *J. Catal.* **1988**, *114*, 259.
(27) Frank, T. C.; Kester, K. B.; Falconer, J. L. *J. Catal.* **1985**, *95*, 396.
(28) Magrini, K. A.; Falconer, J. L.; Koel, B. E. In *Catalyzed Direct Reactions of Silicon;* Lewis, K. M., Rethwisch, D. G., Eds.; Studies in Organic Chemistry Series 49; Elsevier: Amsterdam, 1993; p 249.
(29) Magrini, K. A.; Falconer, J. L. In *Catalyzed Direct Reactions of Silicon;* Lewis, K. M., Rethwisch, D. G., Eds.; Studies in Organic Chemistry Series 49; Elsevier: Amsterdam, 1993; p 265.
(30) Acker, J. Ph.D. Thesis, Freiberg University of Mining and Technology, Freiberg, Germany, 1999.
(31) Acker, J.; Bohmhammel, K.; Roewer, G. In *Silicon for the Chemical Industry IV*; Øye, H. A., Rong, H. M., Nygaard, L., Schüssler, G., Tuset, J. Kr., Eds.; Norwegian University of Science and Technology: Trondheim, Norway, 1998; p 133.
(32) Acker, J.; Bohmhammel, K.; Roewer, G. In *Organosilicon Chemistry IV: From Molecules to Materials*; Auner, N., Weis, J., Eds.; Wiley-VCH: Weinheim, Germany, 2000; p 818.
(33) Nagaki, H.; Simon, A.; Borrmann, H. *J. Less-Common Met.* **1989**, *156*, 193.
(34) Mattausch, H.; Simon, A. *Angew. Chem.* **1998**, *110*, 498.
(35) Mattausch, H.; Oeckler, O.; Simon, A. *Z. Anorg. Allg. Chem.* **1999**, *625*, 297.
(36) Acker, J.; Röver, I.; Roewer, G.; Bohmhammel, K. In *Silicon for the Chemical Industry IV*; Øye, H. A., Rong, H. M., Nygaard, L., Schüssler, G., Tuset, J. Kr., Eds.; Norwegian University of Science and Technology: Trondheim, Norway, 2000; p 121.
(37) Alvarez-Idaboy, J. R.; Mora-Diez, N.; Vivier-Bunge, A. *J. Am. Chem. Soc.* **2000**, *122*, 3715.
(38) Alvarez-Idaboy, J. R.; Mora-Diez, N.; Boyd, R. J.; Vivier-Bunge, A. *J. Am. Chem. Soc.* **2001**, *123*, 2018.
(39) Mora-Diez, N.; Alvarez-Idaboy, J. R.; Boyd, R. J. *J. Phys. Chem.* **2001**, *105*, 9034.
(40) Becerra, R.; Frey, H. M.; Mason, B. P.; Walsh, R.; Gordon, M. S. *J. Chem. Soc., Faraday Trans.* **1995**, *91*, 2723.
(41) Becerra, R.; Boganov, S. E.; Egorov, M. P.; Faustov, V. I.; Nefedov, O. M.; Walsh, R. *J. Am. Chem. Soc.* **1998**, *120*, 12657.
(42) Muench, J. L.; Kruuv, J.; Lepock, J. R. *Cryobiology* **1996**, *33*, 253.
(43) Luo, L.; Zybill, C. E.; Ang, H. G.; Lim, S. F.; Chua, D. H. C.; Lin, J.; Wee, A. T. S.; Tan, K. L. *Thin Solid Films* **1998**, *325*, 87.
(44) McCabe, R. W.; McCready, D. F. *J. Phys. Chem.* **1986**, *90*, 1428.
(45) Frank, T. C.; Falconer, J. L. *Langmuir* **1985**, *1*, 104.
(46) Tamhankar, S. S.; Gorkan, A. N.; Doraiswamy, L. K. *Chem. Eng. Sci.* **1981**, *36*, 1365.
(47) Acker, J.; Bohmhammel, K. *Thermochim. Acta* **1999**, *337*, 187.
(48) Xiao, C.; Hagelberg, F. *J. Mol. Struct.* **2000**, *529*, 241.
(49) Kim, K. H., Park, T. S.; Sohn, K. S.; Kim, S. C. *J. Korean Phys. Soc.* **1987**, *20*, 82.
(50) Tanaka, K.; Saito, T.; Suzuki, K.; Hasegawa, R. *Phys. Rev. B: Condens. Matter* **1985**, *32*, 6853.
(51) Peterson, K. L.; Hsiao, J. S.; Chopra, D. R.; Dillingham, T. R. *Phys. Rev. B: Condens. Matter* **1988**, *38*, 9511.
(52) Nishitani, S. R.; Fujii, S.; Mizuno, M.; Tanaka, I.; Adachi, H. *Phys. Rev. B: Condens. Matter* **1998**, *58*, 9714.
(53) Peterson, K. L.; Hsiao, J. S. *Phys. Rev. B: Condens. Matter* **1988**, *38*, 10911.
(54) Larsson, R.; Folkesson, B. *Acta Chem. Scand.* **1996**, *50*, 1060.
(55) Witusiewicz, V. T. *J. Alloys Compd.* **1994**, *203*, 103.
(56) Witusiewicz, V. T. *J. Alloys Compd.* **1995**, *221*, 74.
(57) Belyi, A. P.; Gorbunov, A. I.; Flid, R. M.; Golubtsov, S. A. *Russ. J. Phys. Chem. (Engl. Transl.)* **1969**, *43*, 637.
(58) Calandra, C.; Bisi, O.; Ottaviani, G. *Surf. Sci. Rep.* **1985**, *4*, 271.
(59) d'Heurle, F. M.; Gas, P. *J. Mater. Res.* **1986**, *1*, 205.
(60) d'Heurle, F. M. *J. Mater. Res.* **1988**, *3*, 167.
(61) Finstad, T. G. *Phys. Status Solidi A* **1981**, *63*, 223.
(62) d'Heurle, F. M.; Peterson, C. S.; Baglin, J. E. E.; La Placa, S. L.; Wong, C. Y. *J. Appl. Phys.* **1984**, *55*, 4208.
(63) Massalski, T. B. *Binary Alloy Phase Diagrams*; ASM Int.: Materials Park, OH, 1990.

(64) Masel, R. I. *Principles of Adsorption and Reaction on Solid Surfaces*; Wiley & Sons: New York, 1996.
(65) Kasdan, A.; Herbst, E.; Lineberger, W. C. *J. Chem. Phys*. **1975**, *62*, 541.
(66) Berkowitz, J.; Greene, J. P.; Cho, H. *J. Chem. Phys*. **1987**, *86*, 1235.
(67) Kalcher, J. *Chem. Phys*. **1987**, *118*, 273.
(68) Nguyen, M. T. *J. Mol Struct.* **1988**, *164*, 391.
(69) Kalcher, J.; Sax, A. F. *J. Mol Struct.* **1992**, *253*, 287.
(70) Mineva, T.; Russo, N.; Sicilia, E.; Toscano, M. *Int. J. Quantum Chem.* **1995**, *56*, 669.
(71) Perrin, J.; Leroy, O.; Bordage, M. C. *Contrib. Plasma Phys*. **1996**, *36*, 3.
(72) Swihart, M. T. *J. Phys. Chem. A* **2000**, *104*, 6083.
(73) Pak, Ch.; Rienstra-Kiracofe, J. C.; Schaefer H. F. *J. Phys. Chem. A* **2000**, *104*, 11232.
(74) Pabst, R. E.; Margrave, J. L.; Franklin, J. L. *J. Mass Spectrom. Ion Phys.* **1977**, *25*, 361.
(75) Gubtsev, G. L. *J. Phys. Chem*. **1994**, *98*, 1570.
(76) Sicilia, E.; Toscano, M.; Mineva, T.; Russo, N. *Int. J. Quantum Chem.* **1997**, *61*, 571.
(77) Ellison, G. B.; Engelking, P. C.; Lineberger, W. C. *J. Am. Chem. Soc*. **1978**, *100*, 2556.
(78) Dixon, D. A.; Feller, D.; Peterson, K. A. *J. Phys. Chem. A* **1997**, *101*, 9405.
(79) Voorhoeve, R. J. H.; Vlugter, J. C. *J. Catal*. **1965**, *4*, 220.
(80) Waltenburg, H. N.; Yates, J. T. *Chem. Rev.* **1995**, *95*, 1589.
(81) Street, R. A. *Hydrogenated Amorphous Silicon*; Cambridge University Press: New York, 1991.
(82) Golubtsov, S. A.; Andrianov, K. A.; Ivanova, N. T.; Turetskaya, R. A.; Podgornyi, I. M.; Feldshtein, N. S. *Zh. Obshch. Khim*. **1972**, *43*, 2000.
(83) Turetskaya, R. A.; Golubtsov, S. A.; Andrianov, K. A.; Eszerets, M. A.; Dzvonar, V. G. *Izv. Akad. Nauk SSSR, Ser. Khim*. **1973**, 394.